Available online at www.sciencedirect.com
SCIENCE DIRECT
Journal of Solid State Chemistry 179 (2006) 1401–1406
JOURNAL OF SOLID STATE CHEMISTRY
www.elsevier.com/locate/jssc

Antiferromagnetic ordering with an anisotropy reversal in $USn_{0.5}Sb_{1.5}$

V.H. Tran*, Z. Bukowski, J. Stępień-Damm, R. Troć

W. Trzebiatowski Institute of Low Temperature and Structure Research, Polish Academy of Sciences, P.O. Box 1410, 50-950 Wrocław, Poland

Received 4 November 2005; received in revised form 26 January 2006; accepted 29 January 2006
Available online 10 March 2006

Abstract

We report on single crystal growth, crystal structure refinements and on the measurements of low-temperature magnetic properties of a novel uranium intermetallic $USn_{0.5}Sb_{1.5}$. Single crystals were grown by means of the antimony flux technique. The crystal structure, refined from single crystal X-ray data, appears to be similar to that of USb_2, i.e., the tetragonal, anti-Cu_2Sb type unit cell with space group $P4/nmm$. Magnetisation and electrical resistivity measurements revealed that this compound orders antiferromagnetically below $T_N = 177(1)$ K. A large magnetocrystalline anisotropy observed in the magnetic properties of $USn_{0.5}Sb_{1.5}$ changes dramatically with decreasing temperature, switching from an easy magnetisation c-axis to an easy ab-plane at 163 K. Due to the opening a superzone gap, the electrical resistivity in-plane shows a small hump just below T_N in a manner resembling the formation of spin-density wave or/and charge-density wave.
© 2006 Elsevier Inc. All rights reserved.

Keywords: Single crystal; Magnetocrystalline anisotropy; Anisotropy reversal; Magnetic and transport properties; Antiferromagnetic ordering

1. Introduction

Uranium dipnictides UX_2 ($X = As, Sb$ and Bi) are subject of intensive investigations over the past four decades [1–11]. These compounds crystallise in a tetragonal, anti-Cu_2Sb-type structure (space group $P4/nmm$) and order antiferromagnetically at relatively high Néel temperatures [1–4]. Furthermore, numerous investigations performed so far on this series of compounds [9,11,12], have revealed that the hybridisation between the $5f$- and sp-electron wave functions is an important factor in determining their physical properties. In fact, effective cyclotron masses m^*, which usually are considered to be a measure of such a hybridisation in f-electron compounds, were found to increase systematically with increasing pnictogen anion radius r_X through the series: $m^* = 4.5m_0$, $6.0m_0$ and $9.2m_0$ for $X =$ As, Sb and Bi, respectively [11]. In other words, the extending of sp-electron wave functions results in strengthening the f–sp hybridisation owing to a broader overlap of the wave functions of the f- and sp-electrons. On the other hand, the increasing of r_X is accompanied with the enlarging the U–U distances. This likely causes the decrease of magnetic interaction between the uranium ions, leading in consequence to the decrease of T_N. Moreover, as suggested by Aoki et al. [11], these UX_2 antiferromagnets offer the possibility to study the so called "dual" nature of the $5f$-electrons. The localised nature of these electrons is reflected by a large value of the ordered moment, while the more itinerant feature is indicated by an enhanced cyclotron mass. In this context, it is worthwhile to investigate the problem how the atom substitution effect influences the magnetic properties of the UX_2 series of compounds. This paper is a report on single crystal growth and crystal structure refinement, and also on the determination of low temperature magnetic properties of a new intermetallic uranium compound $USn_{0.5}Sb_{1.5}$. We have chosen the substitution of Sb by the Sn atoms because such a substitution may cause the decrease in the number of conduction electrons. Thus, we expect that the above substitution goes with the effect of emptying the p-band, which in turn increases the charge transfer from the f-band to the p-band. In consequence, the $5f$–sp hybridisation strength is expected to increase substantially. Apparently, the effect of the Sn substitution may provide an additional disorder effect. However, this would be expected to play a

*Corresponding author. Fax: +48 71 344 1029.
E-mail address: V.H.Tran@int.pan.wroc.pl (V.H. Tran).

0022-4596/$ - see front matter © 2006 Elsevier Inc. All rights reserved.
doi:10.1016/j.jssc.2006.01.072

secondary role compared to the dominant role of the hybridisation process.

2. Experimental details

Single crystals of $USn_{0.5}Sb_{1.5}$ have been grown using an antimony-flux method. A mixture of good quality elements U (purity at. 99.9%), Sn (at. 99.999%) and Sb (at. 99.999%) with the atomic ratio U:Sn:Sb = 1:0.5:10 was placed in an alumina crucible and sealed in an evacuated quartz ampoule. The ampoule was heated with a heating rate of 15 °C/h up to 1080 °C and kept at this temperature for 10 h , followed by cooling down to 600 °C with a step of 2 °C/h. Then the ampoule was cooled down to room temperature with a rate 23 °C/h. The excess of Sb was removed by means of sublimation in high vacuum at 600 °C. The obtained single crystals with typical dimension $3 \times 2 \times 0.1\,mm^3$ were examined by a scanning electron microscope Phillips 515 and an energy dispersive X-ray spectrometer PV9800. Single crystal X-ray diffraction data were collected at room temperature using Xcalibur-CCD diffractometer (MoKα, $\lambda = 0.071073$ nm). The ω scan mode and an exposure time per frame of 30 s were employed. Data reduction and semi-empirical absorption correction were performed using CrysalisRED program [13], while for crystal structure refinements we used a SHELXL-97 program [14]. Measurements of magnetisation, M, were performed in the temperature range 1.7–300 K and in magnetic fields up to 5 T using a Quantum Design Magnetic Property Measurement System SQUID magnetometer. The electrical resistivity ρ was measured in the temperature range 4–300 K using a conventional four-probe DC-technique with a current of 10 mA.

3. Results and discussion

3.1. Crystal structure

The SEM image of the typical grown single crystal is shown in Fig. 1. The surface of the crystal corresponds to the (0 0 1) plane. The results of EDX analysis of several selected crystals are as follows U:Sn:Sb = 33.38:16.06:50.56, yielding the chemical composition around $USn_{0.5}Sb_{1.5}$. The single crystal X-ray pattern could be indexed on the basis of a tetragonal unit cell with space group $P4/nmm$. The starting atomic parameters have been deduced from an interpretation of Patterson plots [15]. In contrast to UT_xSb_2, (T = transition metal) [16,17], adopting the $HfCuSi_2$ structure type [18,19], the studied crystal $USn_{0.5}Sb_{1.5}$ crystallizes in an anti-Cu_2Sb structure type, i.e., the Sn atoms do create a new layer with the $2a$ $(1/4, 3/4, 0)$ position, but share one and/or two available $2b$ $(1/4, 3/4, 1/2)$ and $2c$ $(1/4, 1/4, z_{Sb})$ positions with Sb. Due to the similar scattering factors of Sn and Sb atoms, an initial refinement has been performed for the USb_2 composition. We have taken into account two positional parameters, namely, the z_U and z_{Sb} ones, which are associated with the U atoms at the position $2c$ $(1/4, 1/4, z_U)$ and with the Sb atoms at the second position $2c$ $(1/4, 1/4, z_{Sb})$, respectively. In the next step only the site occupancy factors of Sb and Sn atoms at $2a$ and $2c$ were refined and finally also the occupancy factors with anisotropic displacement parameters were included to the crystal refinement. The final refinement of 2119 observed reflections diverges at reliability factors $R_1 = 0.0371$, $wR_2 = 0.0804$. The crystal data and refinement details are listed in Table 1. The atomic positional parameters, occupancy factors and displacement coefficients are given in Table 2. The refined composition of $USn_{0.5}Sb_{1.5}$ is found to be in good agreement with EDX data although the X-ray analysis has a limited sensitivity towards distinguishing

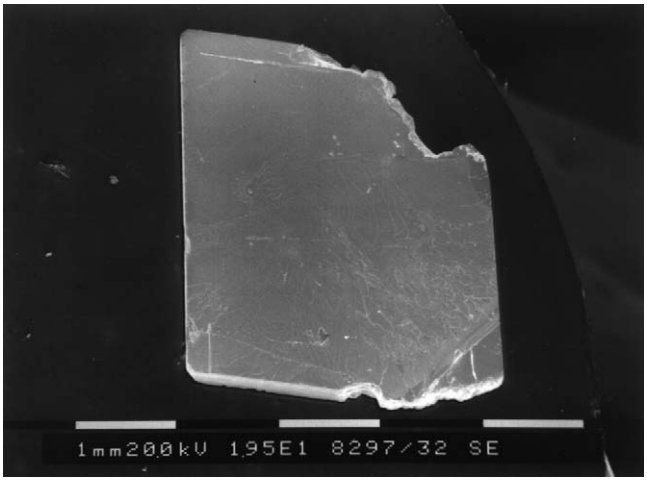

Fig. 1. The SEM image of a $USn_{0.5}Sb_{1.5}$ single crystal.

Table 1
Crystal data and structure refinement for $USn_{0.5}Sb_{1.5}$

Formula weight	480.00
Wavelength	0.71073 Å
Crystal system, space group	Tetragonal, $P4/nmm$
Unit cell dimensions	$a = 4.279(1)$ Å, $\alpha = 90°$
	$b = 4.279(1)$ Å, $\beta = 90°$
	$c = 8.737(2)$ Å, $\gamma = 90°$
	Volume = 159.97(6) Å^3
Z, calculated density	2, 9.965 Mg/m^3
Theta range for data collection	10.24−39.22°
Limiting indices	$-5 \leqslant h \leqslant 4, -5 \leqslant k \leqslant 5, -11 \leqslant l \leqslant 11$
Reflections collected/unique	2119/139 [R(int) = 0.17(5)]
Completeness to theta	4.67–27.71, 99.3 %
Data/restraints/parameters	140/0/12
Refinement method	Full-matrix least-squares on F^2
Data/restraints/parameters	128/0/12
Goodness-of-fit on F^2	1.132
Final R indices [$I > 2\sigma(I)$]	$R_1 = 0.0368$, w$R_2 = 0.0801$
R indices (all data)	$R_1 = 0.0371$, w$R_2 = 0.0804$
Extinction coefficient	0.011(2)
Largest diff. peak and hole	2.086 and −5.522 e Å^{-3}

Table 2
Atomic coordinates, occupations, anisotropic and equivalent isotropic displacement parameters for $USn_{0.5}Sb_{1.5}$

Atoms	Occupation	x, y, z	U(eq)	U_{11}	U_{22}	U_{33}
U	1	0.25, 0.25, 0.7804(1)	13.3 (6)	13.3 (6)	9.4 (6)	12.0 (5)
Sb/Sn	0.76(1)/0.24	0.75, 0.25, 0.5	14.7 (8)	14.7 (8)	9.2 (8)	12.8 (6)
Sb/Sn	0.72(1)/0.28	0.25, 0.25, 0.1407(2)	11.8 (7)	13.8 (7)	10.1 (8)	12.6 (6)

Anisotropic displacement parameters ($Å^2 \times 10^3$) for $USn_{0.5}Sb_{1.5}$. The anisotropic displacement factor exponent takes the form: $-2\pi^2[h^2a^2U_{11} + \cdots + 2hka^*b^*U_{12}]$, $U_{23} = U_{13} = U_{12} = 0$. U(eq) is defined as one third of the trace of the orthogonalised U_{ij} tensor.

Sn and Sb atoms. As is apparent from Table 1, the lattice parameter $a = 4.279(1)$ Å of $USn_{0.5}Sb_{1.5}$ is comparable to that of USb_2 (4.270 Å), but the lattice parameter c is somewhat smaller (8.737(2) Å compared to 8.784 Å [20]). Thus, the observed lowering in the lattice parameter c reflects clearly the influence of the presence of the Sn atoms in the unit cell due to the substitution. This is a quite possible consequence of the difference in atomic radius of Sn and Sb, i.e., 1.40 and 1.45 Å, respectively.

3.2. Magnetic properties

The inverse magnetic susceptibility of $USn_{0.5}Sb_{1.5}$ measured at $\mu_0 H = 0.5$ T and at temperatures above 150 K is displayed in Fig. 2(a). Both the susceptibility components, i.e., those measured perpendicular to the c-axis, $\chi_\perp$, and along the c-axis, $\chi_\parallel$, can be very well fitted just above T_N to the Curie–Weiss law: $\chi(T) = C/T - \Theta_p$, where $C = \mu_0 N_A \mu_{eff}^2/3k_B$. The fits yielded the effective magnetic moment $\mu_{eff} = 3.11$ and $3.58\,\mu_B$, respectively. These values are close to those expected for the free U^{3+} or U^{4+} ions. This implies that the $5f$-electrons in $USn_{0.5}Sb_{1.5}$ are at least at high temperatures localised. Therefore, it is not surprising that the difference in the paramagnetic Curie temperatures $\Theta_\perp$ ($= -37$ K) and $\Theta_\parallel$ ($= 45$ K) is pronounced. This observation points to a huge magnetocrystalline anisotropy existing in the studied compound. A similar behaviour was also observed in the UX_2- and $UTSb_2$-type series [12,16,17].

The magnetic susceptibility data are presented in Fig. 2(b). The sharp maxima in $\chi(T)$ at about 180 K are well evidenced in both the susceptibility components. Tentatively, we have to attribute these maxima to the onset of an antiferromagnetic order. The Néel temperature of $USn_{0.5}Sb_{1.5}$, defined as a maximum in the temperature derivative $d(\chi T)/dT$, amounts to $T_N = 177.0 \pm 0.5$ K. Unexpectedly, T_N of $USn_{0.5}Sb_{1.5}$ is considerably reduced compared to that of USb_2 (203 K [7]). This is unlike to the behaviour, for example, of the series UBi_2–USb_2–UAs_2, where the reduction in the unit cell volume, brings about the opposite tendency of the Néel temperature and in consequence leads to the increase in T_N values, which in turn is usually associated with an increase in the magnetic exchange interactions. In the case of $USn_{0.5}Sb_{1.5}$, the observed reduction of the Néel temperature is due to a considerable increase in the strength of the $5f$–sp hybridisation in comparison to that in USb_2, i.e., the $5f$-electrons in $USn_{0.5}Sb_{1.5}$ are presumably much less localised than those in USb_2.

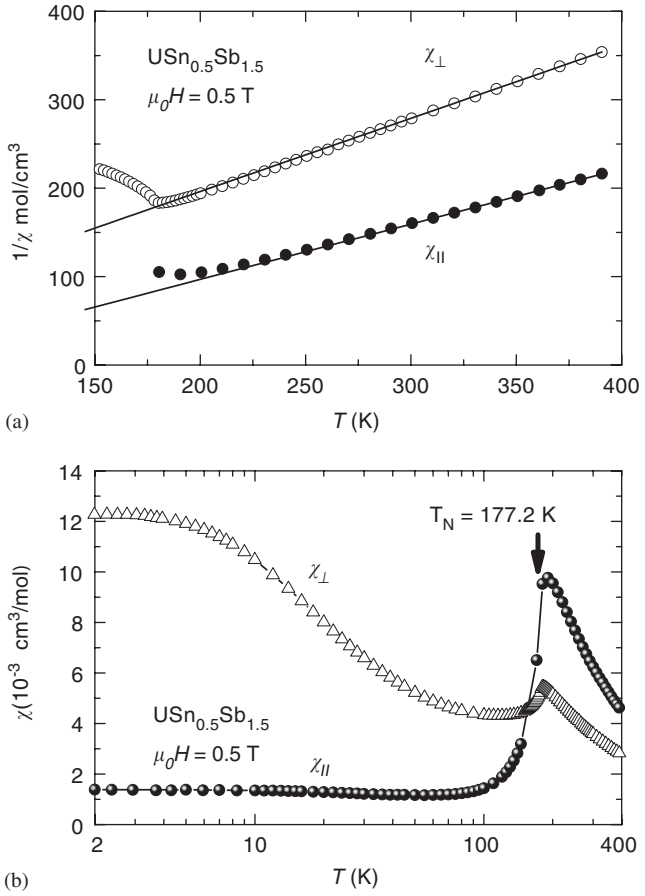

Fig. 2. (a) Temperature dependence of the reciprocal magnetic susceptibility of $USn_{0.5}Sb_{1.5}$ measured perpendicular ($\chi_\perp$) and along ($\chi_\parallel$) to the c-axis. (b) Magnetic susceptibility as a function of temperature.

Inspecting Fig. 2(b), one notes that a reversal in anisotropy appears near 163 K. Below this temperature the $\chi_\perp$ component becomes larger than the $\chi_\parallel$ one. A similar behaviour has already been observed in the UX_2 series [12]. The occurrence of the reversal anisotropy may suggest that the magnetic moments at lower temperatures are aligned closer the ab-plane than along the c-axis. However, this suggestion has to be supported by low temperature neutron diffraction experiments, since the

neutron experiments on the UX_2 ($X = P, Sb$) series have so far been performed at temperatures not lower than 77 K [5,8]. Hence we have not enough data to explain the effect of the anisotropy reversal in $USn_{0.5}Sb_{1.5}$. It seems that the origin of such a behaviour in the investigated material is certainly the result of different kind of anisotropy contributions, e.g., due to the magnetocrystalline anisotropy caused by crystal electric field interactions. In addition, there exists also an exchange anisotropy connected with the anisotropic type of hybridisation [21]. Another behaviour of $\chi_\perp(T)$, which is here worthwhile underlaying is a rapid increase in its values when T goes down to 2 K, the lowest temperature measured. We have no explanation for this behaviour at present.

Magnetisation taken at 1.9 K and in fields up to 5 T is shown in Fig. 3. Since $M_\perp$ is much larger than $M_\parallel$ at this temperature, one can suspect that we deal here with the anisotropy of easy *ab*-plane. In the magnetic field range studied, the magnetisation shows no either any metamagnetic phase transition nor hysteresis. At moderately strong fields above about 3 T, there is apparent a small deviation in $M_\perp(H)$ from the linear dependence, while $M_\parallel$ component having a small magnitude, is almost linear in applied magnetic fields.

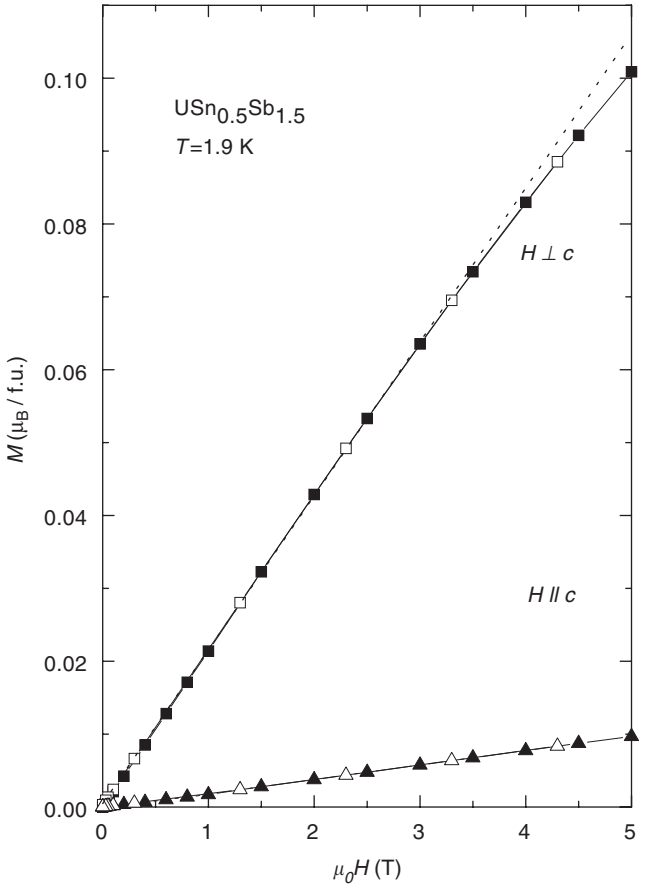

Fig. 3. Magnetisation $M_\perp$ and $M_\parallel$ of $USn_{0.5}Sb_{1.5}$ as a function of applied magnetic field, measured for the magnetic field directed perpendicular and along to the *c*-axis, respectively. The dashed line indicates a deviation of $M_\perp(B)$ from the linear dependence.

3.3. Electrical resistivity

Before having described the electrical resistivity behaviour for $USn_{0.5}Sb_{1.5}$ we would like to recall some important data reported earlier in the literature for USb_2. Henkie et al. [7,10], Aoki et al. [11] and Warzycha [22] have shown that the resistivity of USb_2 is very anisotropic. $\rho_\parallel$ was reported to be considerably larger than $\rho_\perp$. Moreover, the former component exhibits at 98 K, i.e., near $T_N/2$ a broad maximum with a value of 2500 μΩ cm. This maximum has been interpreted as due to a reconstruction of the Fermi surface. Furthermore, the $\rho_\perp$ dependence was reported to follow a $T^{5/2}$ law below T_N. For $USn_{0.5}Sb_{1.5}$ due to flatness of crystals measured we were able to measure only the $\rho_\perp(T)$ component. The obtained data are shown in Fig. 4. The resistivity at room temperature amounts to 209(1) μΩ cm. ρ increases slowly with decreasing temperature until it reaches a broad maximum value of about 210 μΩ cm at 220 K. Below T_N the resistivity shows a step-like increase followed by a maximum at 172 K. A similar feature was observed in numerous antiferromagnets with the superzone gap opening just below T_N [23,24]. In some cases like Cr [25], $NbSe_2$ [26], $NbSe_3$ [27] and URu_2Si_2 [28], such an anomaly was also interpreted as a result of the formation of charge/spin density waves [29]. In

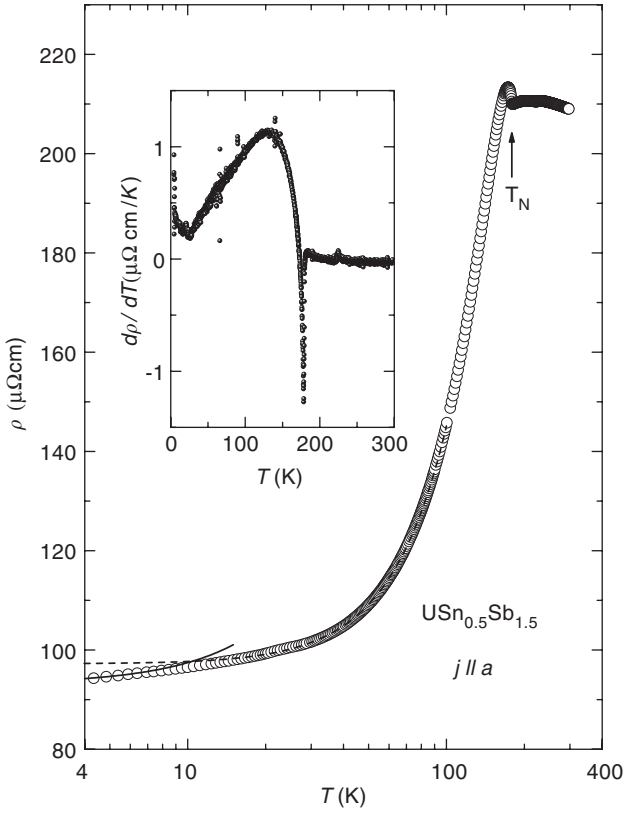

Fig. 4. Temperature dependence of the electrical resistivity for $USn_{0.5}Sb_{1.5}$ measured for the current perpendicular to the *c*-axis. The dashed and solid lines are fits to T^2 and $T^{3/2}$ dependencies, respectively. The inset shows the temperature derivative of the resistivity around the Néel temperature.

the inset of Fig. 4, we show the temperature derivative of the resistivity $d\rho(T)/dT$ for the temperature range close to T_N. The observed in the $d\rho(T)/dT$/curve minimum at 178 K supports the existence of an antiferromagnetic phase transition in $USn_{0.5}Sb_{1.5}$. The difference in the values of T_N accounting up to 1 K, determined from the susceptibility and resistivity measurements seems to be acceptable. With further lowering temperature, the resistivity gradually decreases because of a decrease in the spin-disorder scattering of carriers. Below $T_N/2$ we have tried to fit the resistivity data to the T^2 dependence, that is expected for the electron–electron or electron–magnon scattering processes. However, the resistivity obeys the $\rho(T) = 97 + 0.005T^2$ dependence only in the temperature range 20–85 K, as illustrated by the dashed line in Fig. 4. An attempt to fit experimental data to an equation involved an energy gap in the magnon spectrum has also failed. For the lowest temperature range, we have found a dependence $\rho(T) = \rho_0 + AT^{3/2}$ with $\rho_0 = 93\,\mu\Omega\,cm$ and $A = 0.136\,\mu\Omega\,cm\,K^{-2}$ (solid line in Fig. 4). One must mention that a $T^{3/2}$ dependence of the resistivity has been observed for crystallographically disordered systems, in which short-range magnetic interactions are meaningful [30,31]. This observation seems to be relevant owing to the statistical distribution of the Sn atoms in positions 2*b* and 2*c* for the Sn and Sb atoms. The disorder effect is also supported by a relatively high residual resistivity value, which persists at about $\sim 90\,\mu\Omega\,cm$, as against $\sim 3\,\mu\Omega\,cm$ for USb_2 [11]. A comparison of the resistivity behaviour of the investigated compound with that of USb_2 measured with $J//a$ indicates a significant difference not only in the residual resistivity but also in the overall $\rho(T)$ shape below T_N. In particular, there is lacking of an anomaly in the resistivity for USb_2. Thus, this may point to a considerable modification of the Fermi surface due to the substitution.

4. Conclusions

We have successfully grown single crystals of a new ternary alloy $USn_{0.5}Sb_{1.5}$. The crystal structure type of this material was found to be the same as that of USb_2, i.e., of anti-Cu_2Sb-type structure. We found a statistical distribution of the Sn atoms over the two available positions 2*b* and 2*c* in the unit cell. Furthermore, we have shown that the substitution of Sb with Sn has a significant influence on the physical properties of $USn_{0.5}Sb_{1.5}$. The main observed changes in the properties due to this substitution are as follows: (i) a remarkable decrease in the Néel temperature compared to the parent compound USb_2, (ii) a modification of the Fermi surface in the ordered state and in consequence in the appearance of a small anomaly in the $\rho(T)$ dependence just below T_N, instead of a huge hump observed in $\rho_{\parallel}(T)$ for USb_2. We have also found (iii) a rapid increase in $\chi_{\perp}(T)$ when T is decreased towards 2 K, and (iv) the reversal of anisotropy in the magnetic susceptibility within the antiferromagnetic region of temperatures below 163 K. It turns out that with increasing temperature the anisotropy changes from that in-plane to a uniaxial one. Further works are required to clarify the mechanisms responsible for the anomaly in the resistivity observed just below T_N and for the reversal of anisotropy below 163 K.

Acknowledgments

Financial support from KBN Grant no. 2 PO3B 109 24 is acknowledged. The authors thank R. Gorzelniak and D. Badurski for their technical assistance.

References

[1] W. Trzebiatowski, R. Troć, Bull. Acad. Pol. Sci. Ser. Sci. Chem. 11 (1963) 661.
[2] W. Trzebiatowski, A. Sępichowska, A. Zygmunt, Bull. Acad. Pol. Sci. Ser. Sci. Chem. 12 (1964) 687.
[3] A. Oleś, J. Phys. (Paris) 26 (1965) 561.
[4] W. Trzebiatowski, A. Zygmunt, Bull. Acad. Pol. Sci. Ser. Sci. Chem. 14 (1966) 496.
[5] J. Leciejewicz, R. Troć, A. Murasik, A. Zygmunt, Phys. Stat. Sol. 22 (1967) 517;
J. Leciejewicz, R. Troć, A. Murasik, A. Zygmunt, Phys. Stat. Sol. 24 (1967) 763.
[6] A. Blaise, J.M. Fournier, R. Langnier, M.J. Mortimer, R. Schenkel, Z. Henkie, A. Wojakowski, Inst. Phys. Conf. Ser. 37 (1978) 184.
[7] Z. Henkie, Z. Kletowski, Acta Phys. Pol. A 42 (1972) 405.
[8] R. Troć, J. Leciejewicz, R. Ciszewski, Phys. Stat. Sol. 15 (1966) 515.
[9] G. Amoretti, A. Blaise, J. Mulak, J. Magn. Magn. Mater. 42 (1984) 65 and references therein.
[10] Z. Henkie, R. Maślanka, P. Wiśniewski, R. Fabrowski, P.J. Markowski, J. Alloys Compd. 181 (1992) 267.
[11] D. Aoki, P. Wiśniewski, K. Miyake, N. Watanabe, Y. Inada, R. Settai, E. Yamaoto, Y. Haga, Y. Onuki, Philose. Mag. B 80 (2000) 1517 and references therein.
[12] D. Kaczorowski, R. Troć, in: H.P.J. Wijn (Ed.), Magnetic Properties of Non-metallic Inorganic Compounds based on Transition Elements Landolt-Börnstein, Numerical Data and Functional Relationship in Science and Technology, Group III, vol. 27, subvol. B7, Springer, Berlin.
[13] CrysalisRED, version 1.71, Oxford, 2003.
[14] G.M. Sheldrick, Program for Crystal Structure Refinement, University of Göttingen, Germany, 1997.
[15] G.M. Sheldrick, SHELXS-97, Program for the Solution of Crystal Structures, University of Göttingen, Germany, 1997.
[16] Z. Bukowski, V.H. Tran, J. Stępień-Damm, R. Troć, J. Solid State Chem. 177 (2004) 3934.
[17] Z. Bukowski, D. Kaczorowski, J. Stępień-Damm, D. Badurski, R. Troć, Intermetallics 12 (2004) 1381.
[18] M. Brylak, M.H. Möller, W. Jetschko, J. Solid State Chem. 115 (1995) 305.
[19] D. Kaczorowski, R. Kruk, J.P. Sanchez, B. Malaman, F. Wastin, Phys. Rev. B 58 (1998) 9227.
[20] E. Guziewicz, T. Durakiewicz, M.T. Butterfield, C.G. Olson, J.J. Joyce, A.J. Arko, J.L. Sarrao, D.P. Moore, L. Morales, Phys. Rev. B 69 (2004) 045102.
[21] B.R. Cooper, R. Siemann, J. Appl. Phys. 50 (1979) 1991;
R. Siemann, B.R. Cooper, Phys. Rev. Lett. 44 (1980) 1015.
[22] R. Warzycha, Phil. Mag. B, in press.
[23] R.A. Craven, R.D. Parks, Phys. Rev. Lett. 31 (1973) 383.

[24] T. Takabatake, M. Shirase, K. Katoh, Y. Echizen, K. Sugiyama, T. Osakabe, J. Magn. Magn. Mater. 177–181 (1998) 53.
[25] A.L. Trego, A.R. Mackintosh, Phys. Rev. 166 (1968) 495.
[26] J.A. Wilson, F.J. DiSalvo, S. Mahajan, Adv. Phys. 24 (1975) 117.
[27] N.P. Ong, P. Monceau, Phys. Rev. B 16 (1977) 3443.
[28] T.T. Palstra, A.A. Menovsky, J.A. Mydosh, Phys. Rev. B 33 (1986) 6527.
[29] E. Fawcett, Rev. Mod. Phys. 60 (1988) 209.
[30] N. Rivier, K. Adkins, J. Phys. F 5 (1975) 1745.
[31] J.H. Fluitmant, R. Boom, P.F. de Chatel, C.J. Schinkel, J.L.L. Tilanus, B.R. de Vries, J. Phys. F 3 (1973) 109.